Theor Chem Acc (2007) 117:969–977
DOI 10.1007/s00214-006-0217-y

REGULAR ARTICLE

Investigation of electric-field-gradient-induced birefringence in H_2 and D_2

A. D. Buckingham · Sonia Coriani · Antonio Rizzo

Received: 2 July 2006 / Accepted: 18 October 2006 / Published online: 10 January 2007

Abstract An ab initio computational investigation of the electric–field–gradient–induced birefringence in H_2 and D_2 is presented. The quadrupole moment and all linear and non-linear optical properties contributing to the induced anisotropy of the refractive index are computed by means of Coupled Cluster Singles and Doubles response theory. The latter leads for these systems to Full Configuration Interaction results. Vibrational averaging, centrifugal distortion due to rotation, isotope effects and differences between ortho and para species are also considered.

Keywords Ab initio calculation · Coupled Cluster response theory · Electric–field–gradient–induced birefringence · Quadrupole moment · Ortho and para-hydrogen · Ortho and para-deuterium

1 Introduction

The electric–field–gradient–induced birefringence (EFGB) is the anisotropy in the refractive index (or retardance) observed when plane-polarized light passes through a medium in the z-direction perpendicular to an external electric field gradient $E_{xx} = -E_{yy}$. It originates (primarily) from the interaction of the electric field gradient with the molecular quadrupole moment, resulting in a partial alignment of the molecules in the sample, and (secondarily) from changes in the effective polarizability induced by the electric field gradient. The first effect is temperature-dependent and can be expressed in terms of the molecular quadrupole moment and the molecular electric-dipole polarizability. The second contribution is temperature-independent and determined by higher-order polarizabilities.

For quadrupolar systems, EFGB measurements can be used to determine the molecular quadrupole moment as suggested in 1959 [1], and realized in 1963 by Buckingham and Disch [2] with the determination of the quadrupole moment of CO_2. Since then, EFGB measurements have often been used for determining molecular quadrupole moments.

The original theory of the EFGB effect, valid for non-dipolar systems, was extended to dipolar gases (where the quadrupole moment is origin-dependent) by Buckingham and Longuet-Higgins [3] in 1968, see also Ref. [4]. In 1991 Imrie and Raab [5] used wave theory and the primitive quadrupole moment operator to derive a new expression for the anisotropy of the refractive index in the EFGB experiment. The general form of the equations remained unchanged in their approach, although the particular combination of higher-order polarizabilities differed from that of Ref. [3].

The differences between the two formulations were brought to prominence in recent years by a series of accurate computational studies on different atomic, linear, dipolar and non-dipolar systems [6–9]. In particular, those on CO [6,7] — where the most accurate ab initio

A. D. Buckingham (✉)
Department of Chemistry, University of Cambridge, Cambridge CB2 1EW, UK
e-mail: adb1000@cam.ac.uk

S. Coriani
Dipartimento di Scienze Chimiche, Università degli Studi di Trieste, Via Licio Giorgieri 1, I-34127 Trieste, Italy
e-mail: coriani@units.it

A. Rizzo
Istituto per i Processi Chimico-Fisici del Consiglio Nazionale delle Ricerche, Via G. Moruzzi 1, I-56124 Pisa, Italy
e-mail: rizzo@ipcf.cnr.it

methods were used — showed that only by using the expressions of Buckingham and Longuet-Higgins was one able to obtain results in satisfactory agreement with experiment. This led Raab and de Lange to reanalyze both formulations [10,11], to resolve the discrepancy in favour of Buckingham and Longuet-Higgins' theory and to modify the wave theory [5] so that it agrees with the forward-scattering theory [3].

The effect of quantized rotation on the alignment of quadrupolar molecules in an electric field gradient was considered in Ref. [12]. Unlike the polarization of the electric dipole moments of rigid linear molecules in an electric field E_z, where only the non-rotating ($J = 0$) molecules contribute [13], all rotational states J participate in the alignment in an electric field gradient $E_{xx} = -E_{yy}$. For H_2 at room temperature quantization of the rotation reduces the alignment to about 75% of the classical result [12].

Hydrogen gas under ordinary conditions is a mixture of two kinds of molecules, ortho-hydrogen and para-hydrogen. Normal hydrogen at room temperature (or at STP) contains 25% of the para form and 75% of the ortho form (the "normal" form). The equilibrium ratio of these two forms depends on temperature, but since the ortho form only has odd rotational quantum states J, it cannot be stable in its pure form. In deuterium the ratio of the ortho- and para-forms above the equilibration temperature, which is roughly around 100 K, is 2:1. At low temperatures the para- (ortho-) form prevails in H_2 (D_2) and the response of the two forms to interaction with polarized light and the electric field gradient differs.

In this paper we present a complete computational study of all quantities entering the EFGB of the two-electron systems H_2 and D_2. The use of extended basis sets, and full-configuration interaction (FCI) guarantees benchmark quality of the computed results for the electronic problem. Vibrational and rotational averaging and isotope effects are considered, as well as centrifugal distortion due to rotation and differences between ortho and para forms of both H_2 and D_2.

2 Theory

For a non-dipolar species possessing a threefold, or higher, rotation axis (the 3-axis) the purely electronic, classical equation for the induced birefringence at the equilibrium nuclear separation is [3]

$$\Delta n_e = \frac{2\pi N E_{xx}}{4\pi\epsilon_0}\left(b_e + \frac{2\Delta\alpha_e\,\Theta_e}{15kT}\right) \tag{1}$$

where $E_{xx} = -E_{yy}$ ($E_{zz} = 0$) is the laboratory electric field gradient, N is the number density, T is the temperature, $\Delta\alpha_e = \alpha_{33,e} - \alpha_{11,e}$ is the dipole polarizability anisotropy, $\Theta_e = \Theta_{33,e}$ is the traceless quadrupole moment, and b_e is an appropriate combination of dipole–dipole–quadrupole and dipole–dipole–magnetic dipole hyperpolarizability tensor components, namely

$$b_e = \frac{2}{15}\left\{B_{\alpha\beta,\alpha\beta} - \mathcal{B}_{\alpha,\alpha\beta,\beta}\right\} - \frac{2}{3\omega}\epsilon_{\alpha\beta\gamma}J'_{\alpha,\beta,\gamma} \tag{2}$$

(we refer to Ref. [3] for the sum-over-state expressions for the $B_{\alpha\beta,\gamma\delta}$, $\mathcal{B}_{\alpha,\beta\gamma,\delta}$ and $J'_{\alpha,\beta,\gamma}$ tensors). ω is the (experimental) frequency of the laser probe light. The symbol $\epsilon_{\alpha\beta\gamma}$ indicates the Levi-Civita tensor and implicit summation over repeated indices is assumed here and throughout. Also above and in the following, unspecified symbols refer to fundamental constants in their standard IUPAC notation.

In the response function formalism [14], the above polarizability and hyperpolarizability tensors can be written [6,7,9,15,16]

$$\alpha_{\alpha\beta} = -\langle\langle\mu_\alpha;\mu_\beta\rangle\rangle_\omega \tag{3}$$

$$B_{\alpha\beta,\gamma\delta} = \langle\langle\mu_\alpha;\mu_\beta,\Theta_{\gamma\delta}\rangle\rangle_{\omega,0} \tag{4}$$

$$\mathcal{B}_{\alpha,\beta\gamma,\delta} = \langle\langle\mu_\alpha;\Theta_{\beta\gamma},\mu_\delta\rangle\rangle_{\omega,0} \tag{5}$$

$$J'_{\alpha,\beta,\gamma} = i\langle\langle\mu_\alpha;m_\beta,\mu_\gamma\rangle\rangle_{\omega,0} \tag{6}$$

where μ_α is the electric dipole moment operator, m_α the magnetic dipole moment operator and $\Theta_{\alpha\beta}$ the traceless electric quadrupole moment operator.

The zero-point vibrationally averaged (ZPVA) classical birefringence reads: [12]

$$\Delta n_c = \frac{2\pi N E_{xx}}{4\pi\epsilon_0}\left(b_0 + \frac{2\Delta\alpha_0\,\Theta_0}{15kT}\right) \tag{7}$$

where b_0, $\Delta\alpha_0$ and Θ_0 are the zero-point vibrationally averaged properties, which can generally be written as an integral of the electronic property — computed as a function of the nuclear coordinates R — over the square of the vibrational ground state wave function $|0(R)\rangle$,

$$P_0 = \langle 0(R)|P_e(R)|0(R)\rangle. \tag{8}$$

Assuming that only the ground vibrational state is populated ($hc_0\omega_e >> kT$), and including quantized rotation and centrifugal distortion [12], the above equation is further generalized to

$$\Delta n_{\rm cd} = \frac{2\pi N E_{xx}}{4\pi\epsilon_0}\left\{b_0 + \frac{2\Delta\alpha_0\,\Theta_0}{15kT}\left[1 - \sigma + \frac{8}{15}\sigma^2 + \cdots\right] + \frac{4kT}{hc_0}\frac{B_0}{\omega_e^2}\left(b'_e + \frac{\Delta\alpha'_e\Theta'_e + 2\Delta\alpha'_e\Theta_e + 2\Delta\alpha_e\Theta'_e}{15kT}\right)\right\} \tag{9}$$

where B_0 is the rotational term of the ground vibrational state, ω_e is the fundamental vibrational wavenumber and $\sigma = \frac{hc_0B_0}{kT}$.

For the specific case of a diatomic molecule, the primed quantities Θ'_e, $\Delta\alpha'_e$, b'_e are the derivatives of, respectively, Θ, $\Delta\alpha$ and b with respect to the displacement ξ from the equilibrium nuclear separation r_e – that is, $\xi = \frac{r-r_e}{r_e}$. They arise from the expansion

$$b = b_e + b'_e\xi + \frac{1}{2}b''_e\xi^2 + \cdots \equiv b_e + \left.\frac{\partial b_e}{\partial\xi}\right|_{\xi=0}\xi + \frac{1}{2}\left.\frac{\partial^2 b_e}{\partial\xi^2}\right|_{\xi=0}\xi^2 + \cdots \tag{10}$$

and similarly for the other quantities.

The general (quantum corrected) expression — see also Eqs. (19) and (20) of Ref. [12] — for a gas at equilibrium is

$$\begin{aligned}\Delta n_v = \frac{2\pi NE_{xx}}{4\pi\epsilon_0 Z}\sum_{vJ}\Bigg\{ & b_v + \frac{2\Delta\alpha_v\,\Theta_v}{15kT} \\ & \times\Big[\frac{1}{4} + \frac{3}{4(2J-1)(2J+3)} \\ & + \frac{3}{(2J-1)^2(2J+3)^2}\frac{kT}{hc_0B_v}\Big] \\ & + \left(\frac{B_v^2}{\omega_e^2}\right)\Big\{4(J^2+J)b'_e + (\Delta\alpha'_e\,\Theta_e + \Delta\alpha_e\,\Theta'_e) \\ & \times\Big[\frac{2}{5hc_0B_v}\big(1 + \frac{3}{(2J-1)^2(2J+3)^2}\big) \\ & + \frac{8(J^2+J)^2}{15kT(2J-1)(2J+3)}\Big] \\ & + \frac{4\Delta\alpha_e\Theta_e}{5hc_0B_v}\big(1 + \frac{3}{(2J-1)^2(2J+3)^2}\big) \\ & + \frac{4\Delta\alpha'_e\Theta'_e}{15hc_0B_v}\Big\} + \cdots\Bigg\}\Gamma_{J,I}(2J+1)\exp\Big(-\frac{W^{(0)}_{vJ}}{kT}\Big)\end{aligned} \tag{11}$$

where $P_v = \langle v(R)|P_e(R)|v(R)\rangle$ is the integral over the square of the v-th vibrational state $|v(R)\rangle$ and J is the rotational quantum number. $W^{(0)}_{vJ}$ is the unperturbed energy of the vibrating rotor, which can be written as [17]

$$W_{vJ} = hc_0T_{vJ} = hc_0(G_v + F_{vJ}) \tag{12}$$

where

$$G_v = \omega_e\left(v+\frac{1}{2}\right) - \omega_e x_e\left(v+\frac{1}{2}\right)^2 + \omega_e y_e\left(v+\frac{1}{2}\right)^3 - \cdots \tag{13}$$

is the energy term of the non-rotating molecule,

$$F_{vJ} = B_vJ(J+1) - D_vJ^2(J+1)^2 + \cdots \tag{14}$$

and

$$B_v = B_e - \alpha_e\left(v+\frac{1}{2}\right) + \gamma_e\left(v+\frac{1}{2}\right)^2 \tag{15}$$

$$D_v = D_e + \beta_e\left(v+\frac{1}{2}\right) \tag{16}$$

The partition function Z is

$$Z = \sum_{vJ}\Gamma_{J,I}(2J+1)\exp\Big(-\frac{W^{(0)}_{vJ}}{kT}\Big) \tag{17}$$

$\Gamma_{J,I}$ is a statistical weight factor that accounts for the nuclear spin (I) degeneracy of the system considered. In the specific case of H_2, $\Gamma_{J,I} = 1$ for para-H_2 ($I = 0$, only even J values allowed) and $\Gamma_{J,I} = 3$ for ortho-H_2 (I=1, only odd J values allowed). For D_2, $\Gamma_{J,I} = 3$ for para-D_2 ($I = 1$, only odd J values allowed) and $\Gamma_{J,I} = 6$ for ortho-D_2 (I=0 and 2, only even J values allowed). It should be noted, however, that the quantum effect due to the nuclear spin coupling becomes less important as T increases. As a consequence, in the temperature range usually considered in experimental determinations (roughly 250–550 K) it is safe to compute the birefringence by omitting $\Gamma_{J,I}$ in Eqs. 11 and 17.

At low temperatures (around the boiling point), the equilibrium state of H_2 is almost entirely of the para form. Only the $J = 0$ rotational state (of the ground vibrational state) is populated in para-hydrogen. The quadrupolar contribution to the energy vanishes and the birefringence becomes (see Eq. 11)

$$\Delta n_p = \frac{2\pi NE_{xx}}{4\pi\epsilon_0}\left(b_0 + \frac{2\Delta\alpha_0\,\Theta_0}{45hc_0B_0}\right) \tag{18}$$

i.e. it is finite when $T \to 0$. In pure ortho-hydrogen, on the other hand, all molecules are in the $J = 1$ rotational state, and Eq. 11 reduces to

$$\Delta n_o = \frac{2\pi NE_{xx}}{4\pi\epsilon_0}\left[b_0 + \frac{2\Delta\alpha_0\,\Theta_0}{25}\left(\frac{2}{3kT} + \frac{1}{5hc_0B_0}\right)\right] \tag{19}$$

i.e. the birefringence follows an inverse-temperature law down to very low temperatures. Finally, for the normal mixture of 3 ortho and 1 para at low T:

$$\Delta n_{3:1} = \frac{2\pi NE_{xx}}{4\pi\epsilon_0}\left[b_0 + \frac{\Delta\alpha_0\,\Theta_0}{25}\left(\frac{1}{kT} + \frac{26}{45hc_0B_0}\right)\right] \tag{20}$$

Table 1 H_2 and D_2—electronic property derivatives (in a.u.) and relevant spectroscopic parameters (in cm^{-1}) employed in the determination of the birefringence. FCI results for the given basis set. For comparison reference values are also given for the term values of the two homonuclear molecules [17]

Property	d-aug-cc-pVTZ	d-aug-cc-pVQZ	d-aug-cc-pV5Z	Ref. [17][a]
Θ'_e	0.741716	0.742041	0.742091	
$\Delta\alpha'_e$	4.93115	4.93873	4.94279	
b'_e	−80.3565	−80.3848	−80.3394	
H_2				
$B_e \times 10^{-1}$	6.11252	6.12812	6.13352	6.0853(0)
$\omega_e \times 10^{-3}$	4.51241	4.51256	4.51545	4.40121(3)
$\omega_e x_e \times 10^{-2}$	1.80744	1.79167	1.79019	1.2133(6)
$\omega_e y_e \times 10^{1}$	9.50883	8.53764	8.41049	8.12(9)
α_e	3.57933	3.51152	3.50808	3.062(2)
$\gamma_e \times 10^{2}$	7.16410	7.05320	7.08910	5.7(7)
$\beta_e \times 10^{3}$	4.97932	5.35807	5.43168	−2.7(4)
$D_e \times 10^{2}$	3.73025	3.72839	3.72632	4.71
D_2				
$B_e \times 10^{-1}$	3.04639	3.05491	3.05791	3.0443(6)
$\omega_e \times 10^{-3}$	3.13180	3.13153	3.13358	3.11550
$\omega_e x_e \times 10^{-1}$	6.29692	6.19497	6.18614	6.182
$\omega_e y_e$	−2.30523	−2.36528	−2.37197	0.562
α_e	1.19636	1.18115	1.18144	1.0786
$\gamma_e \times 10^{2}$	0.938625	1.03341	1.08479	1.265
$\beta_e \times 10^{3}$	1.15233	1.23666	1.25274	−0.69
$D_e \times 10^{3}$	9.11501	9.09425	9.08645	11.41

[a] According to the author of [17], "(...)uncertainty may considerably exceed ±10 units of the last decimal place"

In deuterium the situation is reversed, and for pure ortho-deuterium at low T Eq. 18 applies, with the term in $\Delta\alpha_0\Theta_0$ approximately twice as large as in para-hydrogen. For pure para-deuterium, only odd values of the rotational quantum numbers are allowed, $J = 1$ at low T and the birefringence is described by Eq. 19. For normal D_2 (2/3 ortho- 1/3 para-) at low T

$$\Delta n_{2:1} = \frac{2\pi N E_{xx}}{4\pi\epsilon_0}\left[b_0 + \frac{2\Delta\alpha_0\,\Theta_0}{225}\left(\frac{2}{kT} + \frac{59}{15hc_0B_0}\right)\right] \tag{21}$$

3 Computational details

All electronic calculations have been done with DALTON [18]. An equilibrium distance of 1.4 a_0 was used.

The augmented correlation-consistent basis sets of Dunning and coworkers [19–21] x-aug-cc-pVXZ—where x denotes the augmentation level and X the cardinal number—were used throughout for the properties. They constitute a well-established hierarchy of basis sets, which allows us to analyze the convergence of the properties with respect to the valence orbital description (X) and the diffuseness (x) of the basis set. For the equilibrium properties we used all singly and doubly augmented sets up to X = 6, and the triply augmented ones up to X = Q. Only the double augmented sets for X = T, Q, 5 were used for the vibrational averaging, which involved the calculation of the various properties at fourteen interatomic distances between 1.0 and 2.0 a.u. The potential energy curves required in order to determine the vibrational wavefunctions were computed from potential energy values determined in the same interval of interatomic distances for each given basis set.

The vibrational matrix elements required for the determination of the birefringence — that is, the $\langle v(R)|P_e(R)|v(R)\rangle$ integrals — were obtained with VIBROT [22]. The final analysis, including the numerical determination of the relevant property derivatives, cf. Eq. 10, and the calculation of the vibrationally corrected birefringence according to Eqs. 7–20, was performed with MATHEMATICA [23]. The values of the parameters employed in such calculations were those derived from VIBROT and they are given in Table 1. For the full quantum birefringence (see Eq. 11) the summation was carried out over the lowest eight vibrational states of the ground electronic state, including for each vibrational level the lowest seven rotational states. These values should be sufficient for normal conditions for H_2 and D_2, since, as seen from the Raman spectra, the population of states with vibrational and rotational quantum number as high as our largest values is, even at 500 K, negligible. They are not present in any detectable amount, and therefore they would hardly contribute to the birefringence.

The electronic properties were computed at the CCSD level. Since we deal with two-electron systems, the CCSD model gives Full Configuration Interaction (FCI) results within the given orbital basis. All frequency-dependent properties were evaluated for the experimental wavelength of 632.8 nm.

The results are presented in atomic units unless otherwise mentioned. Conversion factors from atomic units to SI and e.s.u. for the quantities of interest are given for instance in Ref. [15].

The tabulated results for the birefringence were obtained for one mole of gas assuming ideal gas behavior at STP, and using an electric field gradient of 1×10^9 Vm^{-2} — the largest electric field gradient strength commonly used in experiment [24]. Thus N was taken as $N = N_A/V_m$, where N_A is Avogadro's constant and $V_m = \frac{N_A kT}{P}$ or, alternatively, $N = \frac{P}{kT}$, where P is the pressure.

The atomic masses used in VIBROT are 1837.15 a.u. for hydrogen and 3671.30 a.u. for deuterium.

4 Results and discussion

4.1 Basis set convergence of the electronic properties

The results of the basis set investigation for the different (purely electronic) contributions to the EFGB for H_2 and D_2 are collected in Table 2. The temperature-dependent term F/T, where $F = \frac{2\Theta_e\Delta\alpha_e}{15k}$, has been evaluated at $T = 297.15$ K to conform to the experimental conditions in Ref. [24].

The results in Table 2, with the exception of the sextuple-zeta values, have already been extensively discussed in Ref. [15], where a comparison with previous computed values for the tensor properties was also carried out. We summarize here the major conclusions of our previous investigation and comment upon the new results.

The x-aug-cc-pVDZ sets are small and clearly inadequate for all properties, as relatively large changes are observed going from the x-aug-cc-pVDZ to the x-aug-cc-pVTZ sets. The quadrupole moment converges smoothly when increasing the quality of the basis set, with the singly augmented sets apparently converging faster. The effect of triple augmentation is rather small from X = T, and becomes irrelevant beyond the X = Q level.

Also the polarizability anisotropy shows a reasonably systematic improvement with the basis set. As already observed in Ref. [15], the d-aug-cc-pVXZ series seems to be the best choice for b and $\Delta\alpha$, whereas it might be sufficient to use a singly-augmented basis set for Θ. In the largest d-aug-cc-pV6Z basis, the quadrupole moment is slightly larger than in the corresponding d-aug-cc-pV5Z set, whereas both the polarizability anisotropy and the absolute value of the b contribution are slightly reduced.

Table 2 Molecular hydrogen—electronic contributions to the molecular properties entering the electric–field–gradient–induced birefringence

Basis set	Θ_e	$\Delta\alpha_e$	$\frac{F}{T}$ [a]	b_e
aug-cc-pVDZ	0.40554	2.2592	129.8	−32.807
aug-cc-pVTZ	0.46041	1.8507	120.7	−36.723
aug-cc-pVQZ	0.45734	1.8624	120.7	−36.920
aug-cc-pV5Z	0.45631	1.8705	120.9	−36.864
aug-cc-pV6Z	0.45632	1.8697	120.9	−36.811
d-aug-cc-pVDZ	0.41119	2.1430	124.9	−36.152
d-aug-cc-pVTZ	0.45793	1.8695	121.3	−37.014
d-aug-cc-pVQZ	0.45641	1.8706	121.0	−36.837
d-aug-cc-pV5Z	0.45612	1.8710	120.9	−36.748
d-aug-cc-pV6Z	0.45627	1.8679	120.8	−36.729
t-aug-cc-pVDZ	0.41124	2.1386	124.6	−36.285
t-aug-cc-pVTZ	0.45781	1.8704	121.3	−37.006
t-aug-cc-pVQZ	0.45633	1.8703	120.9	−36.826

Results in a.u. Wavelength 632.8 nm, $T = 297.15$ K
[a] $F = \frac{2\Theta_e\Delta\alpha_e}{15k}$

4.2 Vibrational effects

Account of the (ro)vibrational effects is mandatory for a sensible comparison of experimental and theoretical results [25]. We collect in Table 3 the ZPVA results for all three molecular contributions to the birefrincence — that is, the quadrupole moment, polarizability anisotropy and hyperpolarizability term — obtained in the d-aug-cc-pVXZ basis sets for X = T, Q, 5.

For H_2 in the d-aug-cc-pV5Z basis, the vibrational effect on the quadrupole moment is of the order of +5.8%, to be compared with the +6% obtained by Bishop and Cybulski [26] at the MP2 level. On $\Delta\alpha$ (in the same basis set) we find +12.4% (cf. +6% for α_{33} and +4% for α_{11} in the static limit at MP2 level by Bishop and Cybulski [26]). On the frequency–dependent b term ZPVA has an influence of around +10% (in

Table 3 H_2 and D_2—zero-point vibrationally averaged molecular properties entering the electric–field–gradient–induced birefringence, obtained according to Eq. 8

	Θ_0	$\Delta\alpha_0$	$\frac{F}{T}$ [a]	b_0
H_2				
d-aug-cc-pVTZ	0.48588	2.1135	145.5	−40.940
d-aug-cc-pVQZ	0.48324	2.1057	144.2	−40.629
d-aug-cc-pV5Z	0.48258	2.1035	143.8	−40.498
D_2				
d-aug-cc-pVTZ	0.47840	2.0450	138.6	−39.837
d-aug-cc-pVQZ	0.47579	2.0379	137.4	−39.533
d-aug-cc-pV5Z	0.47512	2.0357	137.0	−39.401

The vibrational wavefunction was determined using for each basis set the corresponding potential energy. Results in atomic units. Wavelength 632.8 nm for the frequency-dependent properties. $T = 297.15$ K
[a] $F = \frac{2\Theta_0\Delta\alpha_0}{15k}$

Table 4 H_2 and D_2—electronic and vibrational averaged birefringence

Basis	Δn_e	Δn_c	Δn_{cd}	Δn_v
H_2				
d-aug-cc-pVTZ	1.962	2.442	1.651	1.650
d-aug-cc-pVQZ	1.965	2.418	1.636	1.632
d-aug-cc-pV5Z	1.966	2.413	1.633	1.628
D_2				
d-aug-cc-pVTZ	1.962	2.307	1.916	1.922
d-aug-cc-pVQZ	1.965	2.285	1.897	1.903
d-aug-cc-pV5Z	1.966	2.280	1.893	1.899

Results multiplied by a factor 10^{16}. Wavelength $\lambda = 632.8$ nm, $T = 297.15$ K, $E_{xx} = 1.0 \times 10^9$ V m^{-2} and $P = 10^5$ Pa. The values of Δn_{cd} were obtained using the derivatives of the relevant properties in Table 1

absolute value). The same percentage effect was found by Bishop and Cybulski for the frequency-dependent dipole–dipole–quadrupole polarizability $B(-\omega, \omega, 0)$ of H_2 at 632.8, nm [27] and for the Verdet constant [28]. In the static limit, the latter property is related to the main contribution to b [4]. Perturbation theory expressions for the static vibrational dipole–dipole–quadrupole hyperpolarizabilities can be found in Ref. [25]. Bishop and Lam estimated the importance of pure vibrational contributions to the static value of B in hydrogen [29–31], which was found to be "quite significant". One would expect such a contribution to be less important at optical frequencies in analogy with the electric-dipole hyperpolarizabilities in the electro-optic Pockels effect and in the dc-Kerr effect, see for instance Ref. [32]. Pure vibrational corrections have so far been computed for the hyperpolarizabilities entering the b term in the study of the EFGB of CO [6] and Cl_2 [33,34].

In the case of D_2, the percentage effects of vibrational averaging are lower than in H_2; in d-aug-cc-pV5Z they are +4.2% on Θ, +8.8% on $\Delta\alpha$ and +7.2% on b.

We now turn our attention to the EFGB as it results from the different approximations discussed in Sect. 2, see data collected in Table 4. The given results were obtained under the conditions $E_{xx} = 1.0 \times 10^9$ V m^{-2}, $T = 297.15$ K and $P = 10^5$ Pa (ideal gas).

We observe that for H_2, zero-point vibrational averaging increases (in absolute value) the purely electronic anisotropy by ca. 23%, cf. Δn_c vs. Δn_e in Table 4. On the other hand, inclusion of quantized rotation and centrifugal distortion (under the assumption that only the ground vibrational state is populated), reduces the classical average by 32%. Therefore, the electronic value is reduced overall by 17% in the case of molecular hydrogen. This is due to the reduction of the temperature-dependent term. The full quantum treatment of rotation and vibration under the chosen conditions of P and T yields only negligible further contributions: a reduction of Δn_{cd} by 0.3%. For D_2 the effect of zero–point vibrational averaging is ca. +16%, corrected by −17% by quantized rotation and centrifugal distortion (4% reduction — in absolute value — of the equilibrium Δn_e). Again very modest is the effect of the full inclusion of ro-vibrational states, but in this case as a small increase of Δn_{cd}.

4.3 Temperature dependence and comparison with experiment

We illustrate in Figs. 1 and 2 the reciprocal temperature dependence of the EFGB for both H_2 and D_2 in the range from 200 up to 550 K, as it results from the different approximations introduced in Sect. 2. Included in the insets are also the curves estimated for the ortho- and para-forms, and their normal mixtures (3:1 for H_2 and 2:1 for D_2, in favour of the ortho-species) in the low-temperature range between 25 and 60 K.

Due to the inverse temperature dependence of the number density N at constant P, none of the four curves Δn_e, Δn_c, Δn_{cd} and Δn_v exhibits a linear behavior with the inverse temperature. Also, it is worth noting that the purely electronic equilibrium approximation Δn_e, Eq. 1, yields a temperature dependence intermediate between those of the ZPV averaged curve Δn_c, Eq. 7, and of the more elaborate expressions including quantized rotation and centrifugal distortion effects (Δn_{cd}, Eq. 9) and an extended account of vibrational effects and rotational effects (Δn_v, Eq. 11). Therefore, ZPVA yields corrections to the purely electronic estimates going in

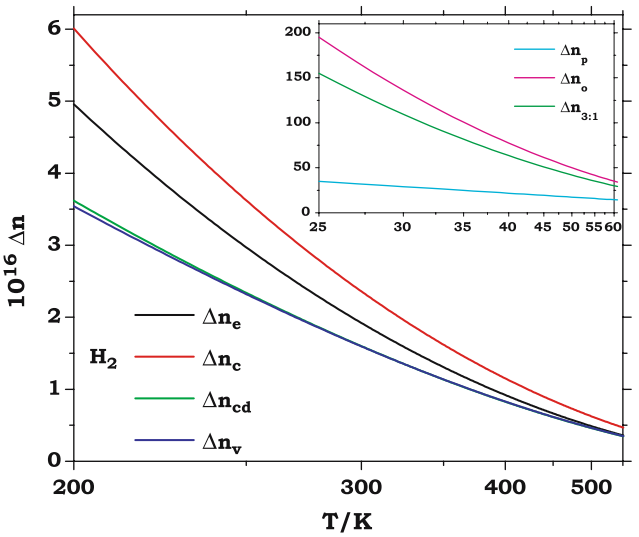

Fig. 1 H_2. Temperature dependence of the electric–field–gradient–induced birefringence at constant pressure computed with the different approximations discussed in the text

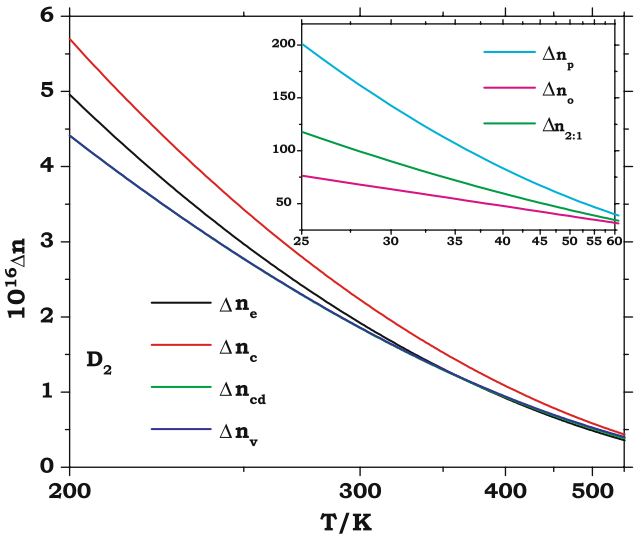

Fig. 2 D_2. Temperature dependence of the electric–field–gradient–induced birefringence at constant pressure computed with the different approximations discussed in the text

the opposite direction to those taken by the more sophisticated approximations including accurate account of the effect of excited vibrational and rotational states of the two molecules in their ground electronic state. Also, the curves traced by Δn_{cd} and Δn_v can hardly be distinguished in the whole range of both Figs. 1 and 2, in particular for D_2. Indeed differences between the two curves would only appear at very low temperatures. Overall, the differences between the four approximations to the temperature dependence of the EFGB are, as expected, larger for H_2 than for D_2.

The curves of Δn_p, Δn_o and of the normal mixtures $\Delta n_{3:1}$ (H_2, Fig. 1) and $\Delta n_{2:1}$ (D_2, Fig. 2) diverge more and more as the temperature approaches the boiling point of the molecule (≈22 K), as can be seen in the insets in the figures. The curves for para-H_2 and ortho- D_2 are straight lines in a reciprocal-T plot at constant P, and for H_2 $\Delta n_{3:1}$ is almost superimposed on the Δn_v curve in the interval of temperatures (inset of Fig. 1). Differences between $\Delta n_{2:1}$ and Δn_v at low temperatures are somewhat larger for the deuterium molecule.

Concerning the comparison between experiment and theory, we collect in Table 5 our best estimates for the various observable quantities which have been the subject of our investigation. For the molecular quadrupole moment Θ of both H_2 and D_2, the best values were obtained adding to the equilibrium value computed in the largest d-aug-cc-pV6Z basis set, the ZPVA correction $(\Theta_0 - \Theta_e)$ obtained in the d-aug-cc-pV5Z set. A similar approach was adopted for the polarizability anisotropy $\Delta\alpha$. From these best values, the tabulated F/T term was computed at $T = 297.15$ K. For H_2, agreement between calculated and "experimental" values is excellent. Also the orientational term F/T derived from our best estimates is in remarkably good agreement with the value given in Ref. [35]: 143.7 vs 146 a.u.

Table 5 H_2 and D_2—best estimates and comparison with the literature (experimental or otherwise) reference values of the molecular quadrupole moment, polarizability anisotropy, temperature-dependent term F/T ($F = \frac{2\Theta\Delta\alpha}{15k}$, $T = 297.15$ K), temperature-independent term b, birefringence Δn and retardance ϕ

Property	Theory	Literature
H_2		
Θ/a.u.	0.48273[a]	0.484[b]
$\Delta\alpha$/a.u.	2.1004[c]	2.12[d]
F/T/a.u.	143.7[e]	146[f]
b/a.u.	−40.48[g]	-46 ± 15[f]
$\Delta n \times 10^{16}$	1.63[h]	1.46 ± 0.24[i]
ϕ/nrad	29[j]	60[k]
D_2		
Θ/a.u.	0.47527	0.483[b]
$\Delta\alpha$/a.u.	2.0326	
F/T/a.u.	136.9	
b/a.u.	−39.38[g]	
$\Delta n \times 10^{16}$	1.90	
ϕ/nrad	34	

Wavelength 632.8 nm. $E_{xx} = 1.0 \times 10^9$ V m^{-2}, $P = 10^5$ Pa
[a] Estimated as Θ_e(d-aug-cc-pV6Z) + [Θ_0(d-aug-cc-pV5Z) − Θ_e(d-aug-cc-pV5Z)]
[b] Recommended value given in Ref. [36], based on the computation of Kolos and Wolniewicz, Refs. [37,38]
[c] Estimated as $\Delta\alpha_e$(d-aug-cc-pV6Z) + [$\Delta\alpha_0$(d-aug-cc-pV5Z) − $\Delta\alpha_e$(d-aug-cc-pV5Z)]
[d] Ref. [39], from light scattering measurements
[e] From the best estimates given previously
[f] From Ref. [35]
[g] Estimated as b_e(d-aug-cc-pV6Z) + [b_0(d-aug-cc-pV5Z) − b_e(d-aug-cc-pV5Z)]
[h] Δn_v(d-aug-cc-pV5Z)
[i] From the value of $\Delta n/(NE_{xx}) = (0.018 \pm 0.003) \times 10^{-36}$ e.s.u. in Ref. [35], recomputed for present simulation conditions (see caption)
[j] At $P = 10^6$ Pa, $T = 300$ K, $E_{xx} = 1.0 \times 10^9$ V m^{-2}, path length $l = 1.8$ m and wavelength $\lambda = 632.8$ nm
[k] Value estimated in Ref. [24] for $P = 10^6$ Pa, $T = 300$ K, path length $l = 1.8$ m, wavelength $\lambda = 632.8$ nm and $E_{xx} = 1.0 \times 10^9$ V m^{-2} from best literature values of $\Delta\alpha$ and Θ, neglecting the temperature-independent term and molecular interactions

A value of the T-independent term b might in principle be obtained, independent of the approximation made, as the limit

$$b = \lim_{T\to\infty} \frac{4\pi\epsilon_0\Delta n}{2\pi N E_{xx}} \tag{22}$$

When applied to the equilibrium and ZPVA expressions for the birefringence, Δn_e and Δn_c, such procedure simply returns the b_e and b_0 values in Eqs. 1 and 7, respectively. The procedure of Eq. 22 fails for both Δn_{cd} and

Δn_v, which, being the result of a perturbative expansion based on the nearly harmonic and nearly rigid rotator approximation, are not appropriate for large values of v and J, and therefore for very high temperatures. The best value for b included in Table 5, and which can thus be regarded as the quantity that more appropriately can be compared with the experiment, is therefore obtained, as for the quadrupole moment and the anisotropy of the electric dipole polarizability, by adding the ZPVA correction $(b_0 - b_e)$ obtained in the d-aug-cc-pV5Z set to the equilibrium value computed in the d-aug-cc-pV6Z basis set. The resulting number can indeed be compared with the value given in the experimental study of Ref. [35]. It is seen that the computed value is remarkably close to the result extracted from experiment on H_2, and it falls well within one standard deviation of the latter. However, the experimentally derived value bears a rather large uncertainty.

The only experimental data for the birefringence Δn are those reported by Buckingham, Disch and Dunmur in 1968 [35], $\Delta n/NE_{xx} = (0.018 \pm 0.03) \times 10^{-36}$ e.s.u. From this value an estimate of $(1.46 \pm 0.24) \times 10^{-16}$ is obtained for Δn, assuming $E_{xx} = 1.0 \times 10^9\,\mathrm{V\,m^{-2}}$, $P = 10^5$ Pa, $T = 297.15$ K, see Table 5. This can be compared with our d-aug-cc-pV5Z value of $\Delta n_v = 1.63 \times 10^{-16}$. Computed and experimentally derived values are in agreement, confirming on one side the validity of the computational approach, and on the other side the quality of the experiment.

The quantity that is actually observed in the laboratory is the retardance ϕ, given by

$$\phi = \frac{2\pi l}{\lambda}\Delta n \tag{23}$$

where l is the path length and λ the wavelength. At 632.8 nm, $P = 10^6$ Pa, $T = 300$ K, $E_{xx} = 1.0 \times 10^9\,\mathrm{V\,m^{-2}}$ and for a path length $l = 1.8$ m, Ritchie and coworkers report an estimate for the experimental retardance of 60 nrad (see Ref. [24] and references therein), obtained from the best available literature values of the quadrupole moment and electric dipole polarizability anisotropy, and neglecting the contribution of the higher order molecular parameters included in b. The author of Ref. [24] writes "However, [the birefringence] of H_2, for which it is known [35] that the temperature-dependent orientational term is only 2–3 times larger in magnitude but opposite in sign to the temperature-independent hyperpolarizability term, is very small and as yet not well determined". We are now in a position to improve on Ritchie's estimate. Assuming the same experimental conditions, and using Eq. 23 with the values of the birefringence given in Table 5, we compute ≈35 nrad using the classical, purely electronic equilibrium expression, ≈43 nrad using the ZPVA expression and approximately 29 from either the quantum expression for the anisotropy, or the one approximated for centrifugal distortion. In the case of D_2 the last value increases to ≈34 nrad. These retardances are ≈ one order of magnitude larger than the limit of detectability of current apparatus, 2 nrad [24].

5 Summary and Conclusions

We have presented a comprehensive ab initio study of the EFGB for the two-electron non-dipolar molecules H_2 and D_2. This optical process has been studied in great detail, by translating into an accurate and extended computational analysis the conclusions of the theoretical formulation of Ref. [12]. "Best values" of the electronic frequency-dependent electric dipole polarizability anisotropy, of the quadratic mixed electric dipole–electric quadrupole–magnetic dipole response functions and of the molecular quadrupole moment of H_2 have been determined employing analytical FCI response theory and extended correlation consistent basis sets. Then the effect of molecular vibrations and rotations has been taken into account, thus allowing for an analysis of the different response of the H_2 and D_2 isotopomers. The potential energy and electronic property curves have been computed for a number of points around the experimental equilibrium internuclear distance, again resorting to FCI analytical response and employing basis sets as large and diffuse as the d-aug-cc-pV5Z, and the derivatives of the electronic properties at the equilibrium distance have been obtained. The vibrational and rotational spectrum of the two isotopomers have then been determined. The matrix elements of the relevant electronic properties over the lowest eight vibrational states of the ground electronic state have been computed. This allowed us to determine a hierarchy of approximations to the EFGB of H_2 and D_2, including first the effect of ZPVA of the electronic properties, then also that of quantized rotation and centrifugal distortion and finally a detailed account of the effect of the excited vibrational and rotational levels.

This procedure has permitted a detailed analysis of the importance of vibrational corrections, at several levels, on the observable. It was also possible to analyze the response of molecular hydrogen at temperatures close to its boiling point, where the gas is entirely in the para-H_2 (or ortho-D_2) form, when subject to linearly polarized radiation in the presence of an electric field gradient. The different approximations which can be employed in such a range of temperatures and applicable to the

para- and ortho- forms, and the resulting birefringence for the normal mixture containing a 3:1 (H_2) or 2:1 (D_2) ratio of ortho/para species, have been analyzed.

It was found that for both H_2 and D_2 species, accounting only for ZPVA of the equilibrium molecular properties as in Δn_c, Eq. 7, worsens the agreement with the results obtained when the effects of quantized rotations are properly accounted for, with respect to the purely electronic equilibrium estimates obtained with Eq. 1, Δn_e. On the other hand, little difference can be found, for both isotopomers at temperatures sufficiently high, between the results obtained when ZPVA is supplemented with proper account of quantized rotation and centrifugal distortion, Δn_{cd}, and those obtained including the effect of all populated rotational and vibrational states, Δn_v.

Overall agreement was obtained between theory and the data existing in the literature extracted from the measurement of the EFGB of H_2 performed in 1968 [35]. We hope that the present study, with its benchmark quality, might help in prompting renewed interest, in particular by experimentalists, in this field, and that soon the results of the present computational study might be accompanied by a definitive experimental determination of the EFGB of molecular hydrogen and molecular deuterium.

Acknowledgments SC thanks Prof. G. L. D. Ritchie for a helpful discussion. She also acknowledges support from the Italian Ministero dell'Università e Ricerca (MUR), Progetti di Ricerca di Interesse Nazionale (PRIN2004).

References

1. Buckingham AD (1959) J Chem Phys 30:1580
2. Buckingham AD, Disch RL (1963) Proc Roy Soc A 273:275
3. Buckingham AD, Longuet-Higgins HC (1968) Mol Phys 14:63
4. Buckingham AD, Jamieson MJ (1971) Mol Phys 22:117
5. Imrie DA, Raab RE (1991) Mol Phys 74:833
6. Rizzo A, Coriani S, Halkier A, Hättig C (2000) J Chem Phys 113:3077
7. Coriani S, Halkier A, Jonsson D, Gauss J, Rizzo A, Christiansen O (2003) J Chem Phys 118:7329
8. Coriani S, Halkier A, Rizzo A, Ruud K (2000) Chem Phys Lett 326:269
9. Coriani S, Halkier A, Rizzo A (2001) In: Recent Res. Devel. Chem. Physics, vol. 2. Pandalai S(ed) Transworld Scientific, Trivandrum, Kerala, India pp 1–21
10. Raab RE, de Lange OL (2003) Mol Phys 101:3467
11. de Lange OL, Raab RE (2004) Mol Phys 102:125
12. Buckingham AD, Pariseau M (1966) Trans Faraday Soc 62:1
13. Van Vleck, JH (1932) The theory of electric and magnetic susceptibilities, sect. 3. Oxford University Press, Oxford
14. Olsen J, Jørgensen P (1995) In: Modern electronic structure theory, Part II. Yarkony DR(ed) World Scientific, Singapore
15. Coriani S, Hättig C, Jørgensen P, Rizzo A, Ruud K (1998) J Chem Phys 109:7176
16. Coriani S, Hättig C, Rizzo A (1999) J Chem Phys 111:7828
17. Huber KP, Herzberg GH (1979) Molecular spectra and molecular structure. Constants of diatomic molecules. Van Nostrand-Reinhold, New York
18. Helgaker T, Jensen HJA, Jørgensen P, Olsen J, Ruud K, Ågren H, Bak KL, Bakken V, Christiansen O, Coriani S, Dahle P, Dalskov EK, Enevoldsen T, Fernández B, Hättig C, Hald K, Halkier A, Heiberg H, Hettema H, Jonsson D, Kirpekar S, Kobayashi R, Koch H, Mikkelsen KV, Norman P, Packer MJ, Pedersen TB, Ruden TA, Sánchez de Merás A, Saue T, Sauer SPA, Schimmelpfenning B, Sylvester-Hvid KO, Taylor PR, Vahtras O (2001) DALTON, an ab initio electronic structure program, Release 1.2 See http://www.kjemi.uio.no/software/dalton/dalton.html
19. Dunning, Jr TH (1989) J Chem Phys 90:1007
20. Kendall RA, Dunning Jr TH, Harrison RJ (1992) J Chem Phys 96:6796
21. Woon DE, Dunning Jr TH (1994) J Chem Phys 100:2975
22. Andersson K, Blomberg MRA, Fülscher MP, Karlström G, Lindh R, Malmqvist PÅ, Olsen J, Roos BO, Sadlej AJ, Schütz M, Seijo L, Serrano-Andrés L, et al. (1997) MOLCAS version 4 Lund University, Sweden
23. Mathematica, v. 5.2, from Wolfram Research
24. Ritchie GLD (1997) In: Optical, electric and magnetic properties of molecules. Clary DC , Orr B(eds) Elsevier, Amsterdam
25. Bishop DM (1990) Rev Mod Phys 62:343
26. Bishop DM, Cybulski SM (1994) J Chem Phys 101:2180
27. Bishop DM, Pipin J, Cybulski SM (1991) Phys Rev A 43:4845
28. Bishop DM, Cybulski SM (1990) J Chem Phys 93:590
29. Bishop DM, Lam B (1987) Chem Phys Lett 134:283
30. Bishop DM, Lam B (1988) J Chem Phys 89:1571
31. Bishop DM, Lam B (1988) Mol Phys 65:679
32. Fernandez B, Coriani S, Rizzo A (1998) Chem Phys Lett 288:677
33. Cappelli C, Ekström U, Rizzo A, Coriani S (2004) J Comp Meth Sci Eng (JCMSE) 4:365
34. Cappelli C, Ekström U, Rizzo A, Coriani S (2005) In: Maroulis G (ed) Computational aspects of electric polarizability calculations: atoms, molecules and clusters. IOS Press, Amsterdam, p. 365, ISBN 1586034952
35. Buckingham AD, Disch RL, Dunmur DA (1968) J Am Chem Soc 90:3104
36. Stogryn DE, Stogryn AP (1966) Mol Phys 11:371
37. Kolos W, Wolniewicz L (1964) J Chem Phys 41:3674
38. Wolniewicz L (1966) J Chem Phys 45:515
39. Bridge NJ, Buckingham AD (1966) Proc Roy Soc (London) A 295:334